Vector Model for Quantitative Susceptibility Mapping (Vector QSM)

Tian Liu[1,2], Cynthia Wisnieff[2,3], Dong Zhou[2], Pascal Spincemaille[2], and Yi Wang[2,3]

[1]*MedImageMetric LLC, New York, NY, United States,* [2]*Radiology, Weill Cornell Medical College, New York, NY, United States,* [3]*Biomedical Engineering, Cornell University, Ithaca, NY, United States*

TARGET AUDIENCE: MRI scientists and engineers interested in magnetic susceptibility.

PURPOSE: Quantitative susceptibility mapping (QSM) has been applied in neuroimaging to elucidate the underlying tissue magnetic susceptibility. However, a scalar susceptibility model may not be sufficient to explain the magnetic field induced by certain types of tissues, such as white matter. Susceptibility tensor imaging (STI) has been proposed (1) to model the field induced by susceptibility tensors, each having six independent parameters. Therefore, STI requires multiple (6~13) scans to fully characterize a tensor map (1-4), making it time consuming and unpractical. In this study, we propose a vector QSM model to account for the field inhomogeneity induced by tensors. Using this model, the right most column of the tensor in the laboratory frame of reference can be resolved from a single scan. Theoretical justifications and *in vivo* evaluations are presented.

THEORY: We first present a special case where the imaging frame coincide with the laboratory frame, and show that the number of unknowns in susceptibility tensor is reduced to 3*N* when the tensors are reduced to vectors, where *N* is the number of voxels. With reduced number of unknowns and regularization, the 3*N* unknowns are recoverable from a single scan providing *N* measured points of the field inhomogeneity. We then generalize the special case to all imaging frames.

Special case: When the imaging frame coincide with the laboratory frame, $H = [0\ 0\ 1]^T$. Considering the field f is a function of $FT\{\chi\}H$, only the right most column of χ has contribution to f, or only the susceptibility vector $[\chi_{13}\ \chi_{23}\ \chi_{33}]^T$ has contribution to f. So f can be expressed as:

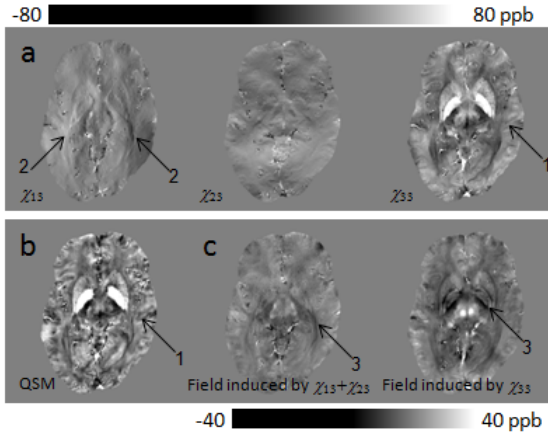

Fig 1. Comparison of scalar and vector QSM.

$$f = FT^{-1}\left[\left(-\frac{k_x k_z}{k^2}\right)FT(\chi_{13}) + \left(-\frac{k_y k_z}{k^2}\right)FT(\chi_{23}) + \left(\frac{1}{3} - \frac{k_z^2}{k^2}\right)FT(\chi_{33})\right] \quad 1$$

To account for spatially varying noise and to select a unique solution, we propose to minimize the following energy function:

$$\{\chi_{13}, \chi_{23}, \chi_{33}\}^* = argmin_{\{\chi_{13},\chi_{23},\chi_{33}\}} \left\| W\left\{ f - FT^{-1}\left[\left(-\frac{k_x k_z}{k^2}\right)FT(\chi_{13}) + \left(-\frac{k_y k_z}{k^2}\right)FT(\chi_{23}) + \left(\frac{1}{3} - \frac{k_z^2}{k^2}\right)FT(\chi_{33})\right]\right\}\right\|_2^2 + \lambda \sum_{i=1}^{3} |M\nabla\chi_{i3}|, \quad 2$$

where λ is the regularization parameter, W is a noise whitening matrix, and M is an edge weighting to allow variations at where tissue interfaces are expected. This energy minimization problem can be efficiently solved using a Newton's method (5).

General case: When the imaging frame does not coincide with the laboratory frame, $H = Q[0\ 0\ 1]^T$ in the imaging frame, where Q is a rotation matrix relating the imaging frame and laboratory frame. In this case, following susceptibility tensor equation, we have:

$$f = FT^{-1}\left\{\frac{1}{3}[0\ 0\ 1]FT(\boldsymbol{\chi}')[0\ 0\ 1]^T - [0\ 0\ 1]\boldsymbol{k}'\frac{\boldsymbol{k}'^T FT(\boldsymbol{\chi}')[0\ 0\ 1]^T}{k'^2}\right\}, \quad 3$$

where $\chi' = Q^T\chi Q$ and $k' = Q^T k$. So the problem is reduced back to the special case if the quantity of interest is χ', the susceptibility tensor in the laboratory frame.

METHODS: *Data acquisition*: MR Datasets from five health subjects were retrospectively analyzed. The imaging was performed on a 3.0-T scanner (HDx, GE Healthcare, Waukesha, WI, USA) with an eight-channel head coil. A 3D multi-echo spoiled gradient echo sequence was used. Imaging parameters were as follows: TEs = 5~50ms with an echo spacing of 5ms; TR = 55 ms; voxel size: from 0.7mm isotropic to 1.2mm isotropic; Bandwidth = 260Hz/pixel, flip angle (FA) = 15°, and parallel imaging with a reduction fraction of two. *Comparison with scalar QSM*: the reconstructed susceptibility vector map was compared with a scalar QSM reconstructed using MEDI (5-7). *Comparison with STI*: One subject was scanned from 12 different head positions. Knowing their rotational matrices Q, a susceptibility tensor map was fitted from the 12 vector QSM images. This susceptibility tensor map was compared with STI (1). A map of eigenvectors (tensor direction map) corresponding to the largest signed eigenvalues of the tensors was displayed in pseudo-color.

RESULTS: The comparison between scalar and vector QSM is shown in Fig. 1. In vector QSM, component χ_{33} reflecting isotropic susceptibility was much greater than χ_{13} and χ_{23}, the anisotropic susceptibility. Compared with scalar QSM, χ_{33} had less variation, especially in the sulcus space (arrow 1). Optical radiation displayed well on χ_{13}, and showed opposite signs on the left and right hemisphere (arrow 2), which was expected from left-right symmetry. We also observed that the field induced by χ_{13} and χ_{23} mainly differentiated white mater from gray matter, while the field map induced by χ_{33} showed gradation in gray matter (arrow 3).

The comparison between vector QSM and STI is shown in Fig. 2. The vector QSM reconstructed from a single orientation showed similarity to the tensor components of the STI using 12 orientations, and appeared to have a higher signal to noise ratio (SNR). Contrary to expectation, the ventricle and the head of caudate nuclei consistently demonstrated anisotropy in both reconstructions (arrows 4&5). The white matter region showed similar colors (mainly left/right red and head/foot) in the tensor direction map.

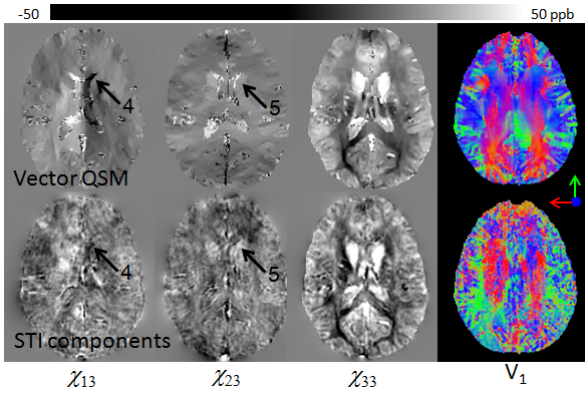

Fig 2. Comparison of vector QSM and STI.

DISUSSION: Although the number of unknowns tripled in vector QSM compared to scalar QSM, they were still resolved using regularization. This is mainly becuase the three convolution kernels relating sources to fields are orthogonal to each other, leading to induced fields with distinct patterns (Fig. 1C). Since vector QSM only requires a single orientation, it can be employed in clinical patients. For example, it is applicable to study multiple sclerosis lesions to differentiate demyelinated lesions from iron-laden lesions. Vector QSM also allows a more efficient reconstruction of STI, using only three acquisitions. Vector QSM also allude to sources other than susceptibility that is responsible for field inhomogeneity in the brain, such as pulsatile flow in the ventricle.

CONCLUSION: We proposed a method for reconstructing vector QSM. This method models the magnetic field better compared to QSM and only requires a single scan. The χ_{33} component also shows less signal variation compared to scalar QSM.

REFERENCES: 1.Liu, C. Magn Reson Med 2010;63(6):1471-7; 2.Li, X *et al*. Neuroimage 2012;62(1):314-30; 3.Wisnieff, C *et al*. Neuroimage 2013;70:363-76; 4.Li, X *et al*. Magn Reson Med 2014; 5.Liu, J *et al*. Neuroimage 2012;59(3):2560-8; 6.de Rochefort, L *et al*. Magn Reson Med 2010;63(1):194-206; 7.Liu, T *et al*. Magn Reson Med 2011;66(3):777-83;